

袁静, 李迎春, 谭桂丽, 等. X射线荧光光谱在地质分析中的若干难点及应用现状[J]. 岩矿测试, 2025, 44(2): 161-173. DOI: 10.15898/j.ykcs.202403150052.

YUAN Jing, LI Yingchun, TAN Guili, et al. Some Difficulties and Status in the Application of X-Ray Spectrometry in Geological Analysis: A Review[J]. Rock and Mineral Analysis, 2025, 44(2): 161-173. DOI: 10.15898/j.ykcs.202403150052.

## X射线荧光光谱在地质分析中的若干难点及应用现状

袁静<sup>1</sup>, 李迎春<sup>2</sup>, 谭桂丽<sup>1</sup>, 黄海波<sup>1</sup>, 张华<sup>1\*</sup>, 刘娇<sup>1</sup>

(1. 中国地质调查局南京地质调查中心, 江苏南京 210016;

2. 国家地质实验测试中心, 北京 100037)

**摘要:** X射线荧光光谱法(XRF)具有无损、快速、环保和分析精度高等特点, 常作为地质样品中主量和微量元素分析的首选方法。然而, 由于地质样品的矿物组成、物理结构特征(如尺寸、形状和分层等)和化学成分(如元素组成、化学形态等)的复杂性与多样性, XRF在地质样品分析的实际应用中存在一些技术难点。本文从小样品量和珍贵样品的分析、XRF的散射效应的应用、易挥发元素分析、变价元素分析和稀有金属分析等方面, 对XRF在地质分析中的难点进行了总结与评述。指出制备易于保存和便于反复测量的小尺寸样片是小样品量和珍贵样品XRF分析的合适方法; XRF散射效应可用于成分未知的样品中更多化学成分信息的获取以及异质性样品原位分析误差的校正; 超细粉末制样、稳定剂的加入和标准加入法建立工作曲线是解决易挥发元素XRF分析困难的方法。认为元素的特征X射线相对强度可用于变价元素价态和形态的分析; 优化校准曲线、降低熔融制样的稀释比、高压激发和改善谱线重叠干扰是解决稀有金属分析困难的有效途径。

**关键词:** X射线荧光光谱; 小样品量和珍贵样品; 散射效应; 易挥发元素; 变价元素; 稀有金属

**要点:**

- (1) 制备便于保存和反复测量的小尺寸样片是XRF定量分析小样品量和珍贵样品的关键。
- (2) XRF散射效应能够为成分未知样品的分析、异质性样品原位分析的误差校正提供有力贡献。
- (3) 超细粉末制样、稳定剂的加入和标准加入法建立工作曲线是利于XRF准确测定易挥发元素的有效方法。
- (4) 采用人工配置的标样或与样品性质相似的二级标样建立并优化工作曲线、降低熔融制样的稀释比、高压激发和改善谱线重叠干扰是解决稀有金属XRF分析难题的有效途径。

中图分类号: O657.34

文献标识码: A

地质类样品(例如天然岩石)被认为是母岩、气候-环境条件和人为条件相互作用的产物<sup>[1]</sup>, 矿物成分和结构变化很大。地质样品的元素定量分析一般采用原子吸收光谱(AAS)、原子荧光光谱(AFS)和电感耦合等离子体质谱/发射光谱(ICP-MS/OES)等方法<sup>[2-4]</sup>。这些湿化学分析方法, 往往需要开放式和高压釜酸分解等复杂且耗时的预处理过程, 并

且在固体样品液化过程中需要使用大量有毒有害的化学试剂。如在开放式酸溶条件下, 低温和常压可能会导致耐酸矿物分解不完全; 高压釜的使用有利于样品分解, 但随之增加了样品污染和损失的风险<sup>[5]</sup>。此外, 酸消化法一个最明显的缺点是不能测量主量元素硅, 因为样品中的硅酸盐被氢氟酸分解而形成易挥发的四氟化硅, 从而导致硅元素的损失。碱熔

收稿日期: 2024-03-15; 修回日期: 2024-07-10; 接受日期: 2024-07-18; 网络出版日期: 2024-09-25

基金项目: 国家重点研发计划项目(2022YFC3705001)课题“岩溶发育特征的快速探测与精细刻画技术和装备研发”; 中国地质调查局地质调查项目(DD20240068)

第一作者: 袁静, 硕士, 高级工程师, 主要从事X射线荧光光谱分析方法的研究与应用。E-mail: candyyj@126.com。

通信作者: 张华, 硕士, 工程师, 主要从事地质实验分析测试工作。E-mail: 191304488@qq.com。

可实现完全分解,但熔融材料必须在酸中重新溶解才能上机测试。

XRF 技术测定地质类样品时采用固体进样,能够有效地避免上述问题<sup>[6-8]</sup>。例如,在测定锡矿石中的锡时<sup>[6]</sup>,采用粉末压片制样,通过加入硼酸、氧化镧降低基体效应和稳定样品总质量吸收系数,建立的分析方法的标准曲线线性良好 ( $R^2=0.9989$ ),测量准确度高 ( $\Delta \lg C < 0.04$ ),精密度良好 (RSD 为 0.39% ~ 1.2%),符合地质样品分析规范要求。又如,测定富硒土壤中的硒时<sup>[7]</sup>,增加按比例混合配置的混合标准物质参与建立校准曲线,解决了硒测定含量范围不足的问题,结果表明高硒土壤样品的 XRF 测定值与 AFS 测定值基本吻合,满足硒含量在 3 $\mu\text{g/g}$  以上的样品的定量分析要求。此外,有研究者将 XRF 技术与其他分析方法结合共同表征矿物的元素含量、物相和矿相组成特征<sup>[8]</sup>。例如,在探究不同产地铜精矿样品的矿物学特征时,XRF 分析发现样品中主要元素为铜、铁、硫和氧,普遍含有锌、硅、铝、镁、钙和铅,通过 Cu/Fe 与 Cu/S 含量比的不同来区分不同产地的铜精矿的物相含量的差异,从而利于进口铜精矿的风险识别和管控。

随着 X 射线光管、探测器等关键技术元件的更新和基体校正方法、计算机技术的进步,XRF 分析方法的检出限不断改善,可测量元素的范围也不断扩大,目前 XRF 技术可对大部分主微量元素 ( $^4\text{Be}\sim^{92}\text{U}$ ,特别是  $^{10}\text{Na}\sim^{92}\text{U}$ ) 进行定性和定量分析,浓度范围可从百分含量到  $\mu\text{g/g}$ ,在岩石学、地球化学、年代学、矿产资源及环境地球科学等领域获得越来越广泛的应用<sup>[9-11]</sup>。然而,由于地质样品的复杂性和测量元素自身的特性,在 XRF 的实际分析中常面临一些难题。本文针对 XRF 在地质样品分析中遇到的若干难点,从小样品量和珍贵样品的分析、XRF 散射效应的应用、易挥发元素分析、变价元素分析和稀有金属分析等方面进行总结与评述。

## 1 小样品量和珍贵样品的分析

地质样品的 XRF 分析中,小样品量和珍贵样品的分析是个难点。如陨石或外星(例如月球)样品等稀有样品;又如带状铁层<sup>[12]</sup>、黄土地层<sup>[13]</sup>样品和斑马岩中周期性带状岩石样品<sup>[14]</sup>,此类样品往往通过微钻探在带状位置打钻获取。在以往的研究中,此类样品往往只能通过扫描电子显微镜、微区 X 射线荧光光谱或激光剥蚀电感耦合等离子体质谱等方法进行定性或半定量分析。若能在小样品量情况下

制成易保存、便于反复测量的样品,将会大大扩展 XRF 在地质领域的应用范围。

有学者尝试了制备小尺寸玻璃熔片解决此类样品的分析问题<sup>[15-16]</sup>。Nakayama 等<sup>[15]</sup>用一种小容量的 Pt-Au 坩埚制备了较小尺寸(12.5mm)的玻璃片,样品和熔剂用量分别为 11mg 和 396mg。结果表明,质量分数 >10% 的分析物, RSD < 3%;质量分数为 1% ~ 10% 的分析物, RSD < 5%;质量分数为 0.1% ~ 1% 的分析物, RSD < 15%,各元素的校准曲线线性均较好(相关系数  $r > 0.998$ )。Ichikawa 等<sup>[16]</sup>提出一种微玻璃珠熔融-XRF 法分析硅质地质样品中的主量元素,样品和四硼酸锂熔剂的用量分别为 1.1mg 和 11mg,制样过程如图 1a 所示。熔融成的微玻璃珠直径约 3.5mm、高度 0.8mm,将微玻璃珠安装在常规大小的空白玻璃样片(直径 35mm)表面(图 1b)待测。研究发现,相较于平坦表面,微玻璃珠的半球面能发射出更强的 X 射线荧光,同时分析结果的 RSD 更小,可能是平坦表面存在气泡且测定平面时半球面与空白玻璃片的粘贴难以完全一致(图 1c)。值得注意的是,由于样品量和分析物尺寸很小,每个样品的荧光强度均弱于传统样片获得的 XRF 强度,使得本来在常规尺寸玻璃片下可忽略不计的干扰线对分析线产生了干扰。如 Cl K $\alpha$  对 Mg K $\alpha$  的干扰、来自于靶材的 Rh L $\gamma_2$  和 Rh L $\gamma_3$  对 K K $\alpha$  的干扰、K K $\beta$  对 Ca K $\alpha$  的干扰等,此时选择细准直器(150 $\mu\text{m}$ )测量 Mg K $\alpha$ 、K K $\alpha$  和 Ca K $\alpha$  能取得较好效果。校准曲线相关系数  $r > 0.997$ ,准确度 (< 5%)和重现性 ( $\geq 95\%$ ,  $n=10$ )表现优异。

不同种类的元素可采用不同的制样方法。例如,Gazulla 等<sup>[17]</sup>在小样品量情况下,针对不同元素分别开发了熔片法(针对主量元素)和压片法(针对氯和硫等易挥发元素)以保证既不浪费样品又能达到最佳分析效果。经条件实验,熔融法的最佳制备条件为: 0.015g 样品(比常规熔片法样品量缩小 30 ~ 40 倍),稀释比 1 : 10,脱模剂 0.20mL。压片法的最佳制备条件为: 0.1000g 样品(比常规压片法样品量缩小约 100 倍)和 0.25mL 黏结剂(17% 甲基丙烯酸正丁酯的丙酮溶液)。用标准物质 SRM98b 和 GBW03103 对熔片法进行不确定度评估,用 GBW03104 和 GBW07407 对压片法测定氯进行不确定度评估,用 BCS-CRM381 和 SRM2709 对压片法测定硫进行不确定度评估,发现标样的测量平均值与推荐值的绝对偏差  $\Delta_m$  均低于扩展不确定度  $U_{\Delta m}$ ,说明分析结果与推荐值之间不存在显著性差异。

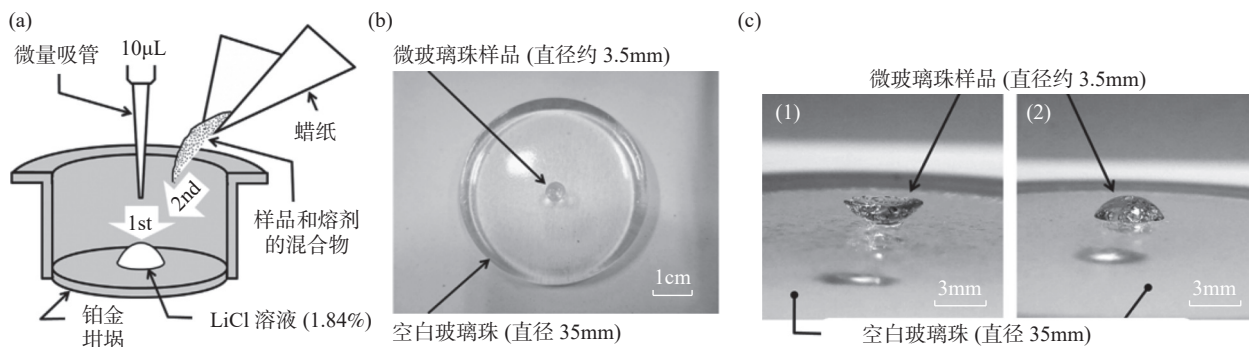


图1 (a) 制备微玻璃珠试样时, 将混合粉末放置在 Pt-Au 坩埚中的工艺原理图; (b) 用硅胶聚合物黏合剂将微玻璃珠 (直径约 3.5mm) 安装在直径 35mm 的空白玻璃片上; (c) 附着在 35mm 空白玻璃片上的微玻璃珠的两个表面: (1) 平面; (2) 半球面。修改自文献 [16]

Fig. 1 (a) Schematic diagram of process to place the mixture powder in a Pt crucible for preparation of a micro glass bead specimen; (b) Top-view photograph of the micro glass bead (approximately 3.5mm diameter) after mounting on the 35mm glass bead blank using silicone polymer adhesive; (c) Comparison of the two available analytical surfaces of the micro glass bead attached on the 35mm glass bead blank: (1) Flat-surface and (2) Hemispherical-surface. Modified from the reference [16].

## 2 X 射线荧光光谱散射效应的应用

康普顿散射 (Compton scattering) 和瑞利散射 (Rayleigh scattering) 能够提供基体和电子密度信息 [18]。康普顿散射与瑞利散射强度的比值 ( $I_{Co}/I_{Ra}$ ) 与原子序数 ( $Z$ ) 有很好的关系 [19]。在实际分析中, XRF 的散射效应可用于解决地学分析中两方面的难题: ①获得成分未知的样品中更多关于化学成分的信息; ②校正异质性样品原位分析的误差, 使感兴趣元素的分析结果更为准确。

### 2.1 成分未知样品的分析

在相同的几何条件和相同的能量下, 对成分未知的样品进行研究时,  $I_{Co}/I_{Ra}$  与  $Z$  的校准曲线可提供重要信息。这种方法首先需要评估已知化学成分的参考物质的  $Z$  与  $I_{Co}/I_{Ra}$  的对应关系, 进而通过从样品谱图中提取的散射线强度信息间接地得出分析元素的浓度 [19]。该方法对于轻基体尤为敏感, 因此对于平均原子序数略有差别的轻元素, 可在不评估其特征 X 射线的情况下, 而是通过比较  $I_{Co}/I_{Ra}$ , 将它们区分开来。此外, 使用  $I_{Co}/I_{Ra}$  的一个实际优点是, 在相同的散射几何条件但不同的仪器参数下 (如管电流、采集时间和探测器接受角), 可比较不同样品的 XRF 谱线, 而无需进一步归一化。因此, 可在相同的实验条件下安排测量任何成分未知或部分未知的样品, 并很快得出相应元素的平均原子序数。

Hodoroaba 等 [19] 通过选择一组平均原子序数  $Z$  在 5 ~ 29 之间的参考物质建立  $I_{Co}/I_{Ra}$  与  $Z$  的校准曲线 (图 2)。随着  $I_{Co}/I_{Ra}$  的降低, 平均原子序数逐渐

增大, 在平均原子序数范围约 10 以内,  $Z$  对  $I_{Co}/I_{Ra}$  的高灵敏度清晰可见, 非常利于推测样品中化学成分信息。例如, C 和 O 的荧光产额很低, 极弱的激发和高能量范围的光谱韧致辐射背景的重叠干扰, 往往使 C、O 等轻元素的谱线被淹没。但通过计算 Rh  $K\alpha$  散射峰的  $I_{Co}/I_{Ra}$  可得到样品的平均原子序数, 从而推算出样品中  $TiO_2$  添加剂的浓度 [19]。又如, 不同的托帕石样品 XRF 光谱中, 可以清楚地观察到

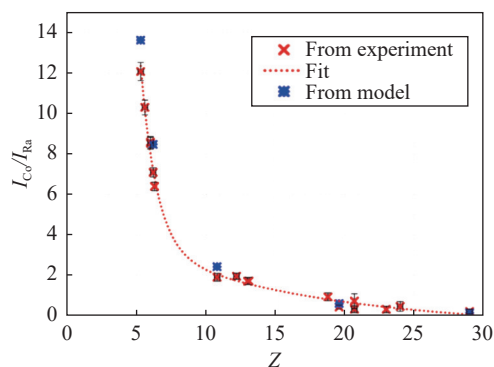


图2 在 45kV, 用多毛细管 X 射线光学仪器在散射角为  $155.5^\circ$  的几何结构下, 用 Rh 靶 X 射线管激发获得的康普顿散射与瑞利散射强度比 ( $I_{Co}/I_{Ra}$ ) 与平均原子序数 ( $Z$ ) 的校准曲线。修改自文献 [19]

Fig. 2 Calibration curve for the Compton-to-Rayleigh intensity ratio ( $I_{Co}/I_{Ra}$ ) versus mean atomic number ( $Z$ ) for an excitation with a Rhodium anode X-ray tube, at a high voltage of 45kV, using polycapillary X-ray optics and under a geometry with a scattering angle of  $155.5^\circ$ . Modified from the reference [19].

Al K 线和 Si K 线荧光信号,但无法检测 O 和 F 的信号(图 3a),而通过计算两个光谱的  $I_{Co}/I_{Ra}$  而推测样品中 F 含量(图 3b),  $I_{Co}/I_{Ra}$  较小的托帕石样品对应较高的平均原子序数,说明 F 离子含量较高<sup>[19]</sup>。

## 2.2 异质性样品原位分析的基体校正

天然地质样品往往由于样品大小、形状变化等因素引起结构不均匀,更如包裹体等特殊样品具有强异质性,XRF 散射效应经常被用于校正样品异质性带来的误差。通常情况下,采用康普顿或者瑞利散射对具有相似基体的样品进行基体校正是有效的,但在多个基体的界面样品中,简单地使用康普顿散射或瑞利散射难以达成理想的效果,因此需要对散射基体校正方法进行改进。

在研究苔藓植物-土壤-岩石界面样品的元素分布特征时,Shen 等<sup>[20]</sup>采用不同散射线校正方法(Com; Ray; Ray/Com; Ray×Ray/Com)校正界面样品的不同基体的感兴趣元素计数,并用校正后的数据与其对应的 ICP-MS 测定值进行线性回归,发现 Ray/Com 校正方法校正  $K_{K\alpha}$  能取得较好效果,而 Ray×Ray/Com 校正方法则适合校正  $Ca_{K\alpha}$ 、 $Mn_{K\alpha}$ 、 $Fe_{K\alpha}$ 、 $Cu_{K\alpha}$ 、 $Zn_{K\alpha}$  和  $Pb_{L\alpha}$ 。采用各自适合的方法校正后,发现界面样品中 K、Ca、Pb、Zn 和 Cu 的谱线在土壤层达到最大峰值,这一结果更接近真实的元素分布规律。该研究是将 XRF 技术应用于感兴趣元素的生物地球化学界面过程的有益探索。

## 3 易挥发元素的分析

碳、硫和卤族元素等挥发性元素,无论采用熔片

法还是压片法都具有一定的难度。采用熔融制样往往会导致测量值偏低;若采用粉末压片制样,则易受到矿物效应和粒度效应的影响。

有学者采用超细粉末压片制样,降低样品的粒度效应和不均匀效应<sup>[21]</sup>。例如,彭桦等<sup>[22]</sup>对沙特阿拉伯磷矿进行超细加工(样品平均粒径为 2~5 $\mu\text{m}$ ),再用 XRF 分析氯、氟等元素,结果显示不同浓度梯度标准物质 Cl 和 F 的测定值与参考值基本吻合,两个内部管理样氯和氟的 RSD( $n=10$ )分别为 5.50%、5.70% 和 2.81%、2.55%,重现性良好。曾江萍等<sup>[23]</sup>用超细粉末压片 XRF 法分析铬铁矿中包括硫元素在内的多元素,样品粒度基本在 10 $\mu\text{m}$  以下,发现硫的分析精密度和准确度均不低于化学法。在该作者的另一项研究中,用超细粉末压片 XRF 法分析磷矿石中的氟,发现不同浓度梯度的测定结果与参考值均吻合,并且该方法将氟元素的测定范围上限提高至 10.68%<sup>[24]</sup>。李小莉等<sup>[25]</sup>用超细粉末压片 XRF 分析碳酸岩中碳、硫等元素,发现当样品粒度达到  $D_{95}<8\mu\text{m}$  时,样品的粒度效应对测量结果的影响基本可以消除。以上研究均表明,超细加工令样品粒径变小,并且粒度分布变窄,特别是大粒度部分骤然减少,能够有效地克服粒度效应的影响,从而降低分析结果不确定度。

熔片法测定硫时,可通过加入稳定剂(如 BaO)来抑制样品在高温熔融过程中硫的挥发。例如,Gazulla 等<sup>[26]</sup>在研究熔片法测定地质样品中的硫时,发现不添加 BaO 时,硫的响应值与硫的浓度校准曲线线性较差(图 4a),不能用于硫的定量分析;而当加

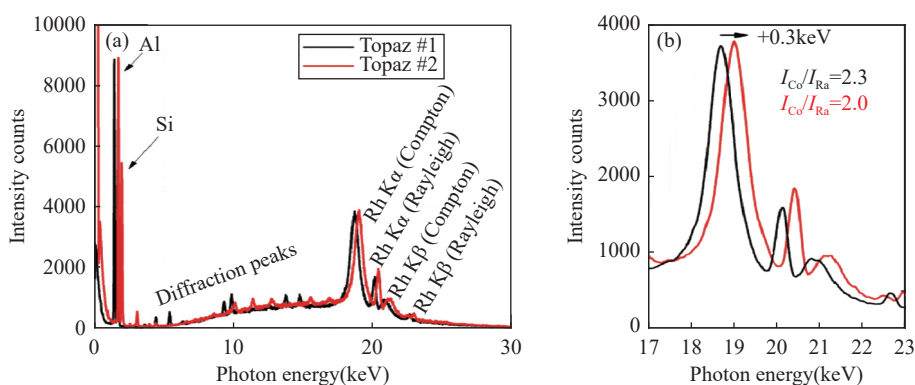


图3 在相同的实验条件下测量了两种托帕石晶体的 XRF 光谱(a)。为了更好地呈现散射线的细节,将 17keV 到 23keV 的区域(b)放大显示,对应托帕石 2 的谱线平移到更高能量 0.3keV 处。修改自文献<sup>[19]</sup>

Fig. 3 XRF spectra of two topaz crystals measured under the same experimental conditions (a). For better visibility of the details of the scattering contributions, a magnified region from 17keV to 23keV is shown (b). Note that the energy scale corresponding to the topaz 2 spectrum has been shifted to higher energies by 0.3keV. Modified from the reference<sup>[19]</sup>.

入两倍于沉淀硫所需 BaO 的化学计量时,校准曲线线性大大改善(图 4b)。采用有证标准物质 SRM1835、SRM2709、GBW03118 和 GBW03122 进行方法验证,测量值与认证值吻合较好,说明稳定剂的加入有效地抑制了硫的挥发,提高了熔片法分析硫的准确度。

溴是古气候研究的一个非常有价值的地球化学指标,但具有溴元素推荐值的标准物质很少,因此校准曲线的建立是 XRF 分析溴的难点。Li 等<sup>[27]</sup>通过标准加入法制定了一系列具有适当浓度的标准物质,建立工作曲线分析海洋地质样品中溴等卤族元素,并用 Rh K $\alpha$  康普顿峰作内标提高溴的分析精度。结果表明,方法精密度 $<5\%$ ,未参与校准曲线回归的标准物质的测量值与推荐值吻合较好,计数时间为 100s 时溴的检出限为  $0.5\mu\text{g/g}$ 。在以往的 XRF 分析中,往往需要 1g 及以上的样品(1g<sup>[28]</sup>、2g<sup>[29]</sup>、4g<sup>[27]</sup>、5g<sup>[30]</sup>)以保证压片具有足够的厚度。有研究者尝试采用全反射 X 射线荧光光谱(TXRF)技术来改善这一局限, TXRF 技术可用非常少的样品量(mg 级)并且采用内部标准方法进行定量。Pashkova 等<sup>[31]</sup>将 20mg 沉积物样品制备成固体悬浮液,用 TXRF 技术采用内标法分析其中的溴,并对比了 TXRF 和波长色散 X 射线荧光光谱(WDXRF)方法的分析结果。发现两种方法的测量值与参考值均吻合较好,而 TXRF 法检出限( $0.4\mu\text{g/g}$ )优于 WDXRF 法的检出限( $1\mu\text{g/g}$ )。

#### 4 变价元素的分析

元素的特征 X 射线的谱峰位置、谱线形状和相对强度可受到原子价态和配位状态的影响,通过观

察此类谱峰参数能够有效地识别元素价态、配位键等信息,并进一步应用于各类地质规律的探索 and 发现<sup>[32-33]</sup>。

岩石矿物样品中铁价态通常用来确定岩浆中的氧活度和矿物与硅酸盐熔体之间的平衡。铁的 XRF 发射谱线的相对强度取决于铁在矿物中的价态,基于此,有研究者用铁的  $K\beta_5/K\beta_{1,3}$  谱峰相对强度作为分析参数分析火成岩中二价铁(FeO)的含量<sup>[32]</sup>,发现对于 FeO 含量 $<1.5\%$ 和  $R^C < 0.2$  的火成岩样品 [ $R^C = C(\text{FeO})/C(\text{Fe}_2\text{O}_3^{\text{Tot}})$ , FeO 与全  $\text{Fe}_2\text{O}_3$  含量比],二价铁含量的测定误差可能 $>20\%$ ,火成岩中酸性成分 FeO 含量的测定误差可能 $>30\%$ ,火成岩碱性岩石 FeO 含量的测定误差可能 $>50\%$ 。而当火成岩中超基性岩、基性岩和中间成分 FeO 的含量 $>1.5\%$ 时,相对误差在 10% 以内,与滴定法分析相当。因此该方法可用于 FeO 含量 $>1.5\%$ 的火成岩中基性、超基性和中间成分的二价铁含量分析。

锰价态和形态的确定可以评估矿物形成过程的氧态、诊断矿物成因和评估矿床潜力,以进一步规划合理的选矿方案。Chubarov 等<sup>[33]</sup>用德国布鲁克 S8Tiger 型波长色散 XRF 分析各类锰矿石中锰的价态和形态,发现  $\text{Mn } K\beta_5/\text{Mn } K\beta_{1,3}$  和  $\text{Mn } K\beta'/\text{Mn } K\beta_{1,3}$  强度比受锰的形态影响最小,但易受到  $\text{Fe } K\alpha_{1,2}$  重叠干扰的影响。 $\text{Mn } K\beta'/\text{Mn } K\beta_{1,3}$  强度比受  $\text{Fe } K\alpha_{1,2}$  重叠干扰的影响最小,但明显依赖于锰的形态。对于含铁较低的样品,用  $\text{Mn } K\beta_5/\text{Mn } K\beta_{1,3}$  评估的误差最小;推荐  $\text{Mn } K\beta_5/\text{Mn } K\beta_{1,3}$  用作评估碳酸盐锰的存在; $\text{Mn } K\beta'/\text{Mn } K\beta_{1,3}$  通常用作评估氧化锰的存在。该方法的优点是不需要复杂的样品处理过程,即可快速地分析锰价态和形态以评估锰矿石质量。

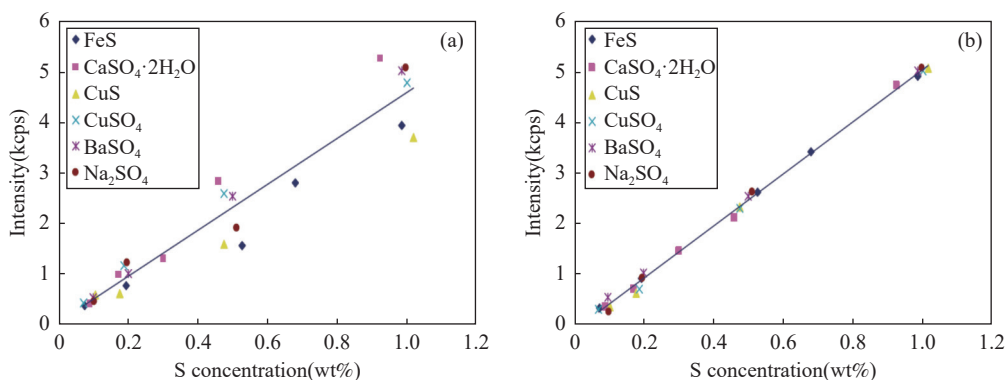


图4 玻璃样片中硫的校准曲线 (a) 未加入 BaO 熔融和 (b) 加入 BaO 作为稳定剂熔融<sup>[26]</sup>

Fig. 4 Calibration curves for sulfur with samples prepared in the form of beads without BaO addition (a) and with BaO addition (b)<sup>[26]</sup>.



Hf  $L\alpha_1$  和 Ta  $L\alpha_1$  线荧光强度的 3~4 倍, GBW07405 中铜的浓度远远高于钽和铌, 因此该文中三种元素方法检出限相同这一结论显然是值得商榷的。此外, 该方法 GBW07405 中钽的测定值为 15mg/kg(推荐值为 8.1mg/kg), 铌的测定值为 3.8mg/kg(推荐值为 1.8mg/kg), 两种元素的测定值和推荐值之间均存在显著性差异。

有学者在测定岩石中钽、铌等稀有金属时则充分考虑了谱线重叠干扰的影响<sup>[42]</sup>。首先, 通过标准物质 CRM-MA-N 研究钽和铜的谱线干扰(图 5 中 a 和 b)。显而易见, Ta  $L\alpha_1$ (0.1522nm) 和 Cu  $K\alpha_1$ (0.1541nm) 之间存在谱线重叠干扰, 而岩石中铜含量常常远高于钽, 因此 Ta  $L\alpha_1$ (0.1522nm) 作为分析线并不是最好的选择。对于 Ta  $L\beta_{1,2}$ (0.1327nm), 其干扰谱线主要有: Ga  $K\beta_{1,2}$ (0.134nm)、Zn  $K\beta_1$ (0.1295nm)、Nb  $K\beta_2$ (0.1331nm)、W  $L\beta_1$ , 而镓、铌和钨在岩石中通常含量较低, 因此选择了 Ta  $L\beta_{1,2}$  作为钽的分析线, 并扣除 Zn  $K\beta_1$  尾峰的干扰。同理, 选择了 Cs  $L\alpha_1$  作为铌的分析线。根据“可忽略误差”标准和  $t$  检验, 钽和铌的测量偏差均不显著, 钽和铌的检出限分别为 2.6mg/kg 和 3.4mg/kg, 将不同成分的岩石样品中钽的 XRF 测定数据与 ICP-MS 数据进行比较, 相关系数为 0.973, 同样证实了分析方法的可靠性。

以上研究表明, 测定稀有金属时, 是否考虑谱线重叠干扰直接影响着分析结果准确度。

## 6 结论与展望

X 射线荧光光谱技术发展至今, 无论从激发源、探测器、样品制备、基体校正和计算方法等方面都取得了长足的发展, 在地学领域得到广泛应用, 特别是曾经难以解决的一些难点如小样品量和珍贵样品分析、成分未知和异质性样品的分析、易挥发元素分析、变价元素分析和稀有金属分析等都取得可观有效的成果。

然而, XRF 技术在地质分析中的应用限制和挑战依然突出: ①分析结果的准确性依赖标准物质,

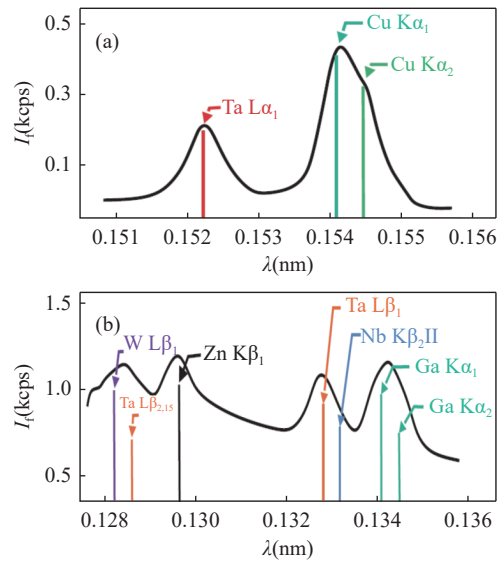


图5 (a) 波长 0.151~0.156nm 的 X 射线荧光光谱谱图 (CRM-MA-N 元素含量: Ta 290mg/kg, Cu 140mg/kg); (b) 波长 0.128~0.136nm 的 X 射线荧光光谱图 (CRM-MA-N 元素含量: Ta 290mg/kg, Ga 59mg/kg, Zn 220 mg/kg, W 70mg/kg, Nb 173mg/kg)。修改自文献<sup>[42]</sup>

Fig. 5 (a) X-ray spectrum within the range of wavelengths from 0.151nm to 0.156nm. CRM-MA-N with the elemental contents: Ta 290mg/kg, Cu 140mg/kg; (b) The spectral distribution within the range of wavelengths from 0.128 to 0.136nm. CRM-MA-N with the elemental contents: Ta 290mg/kg, Ga 59mg/kg, Zn 220mg/kg, W 70mg/kg, Nb 173mg/kg. Modified from the reference<sup>[42]</sup>.

尤其对于成分复杂的地质样品, 需要物理化学性质类似的样品参与校准曲线的绘制; ②对于  $Z \leq 8$  的轻元素仍难以定量测定。未来随着粒子物理学、光学系统以及探测装置等技术的进步, 相信这些局限将会逐渐被攻克。此外, 近年来随着地球科学融合发展的趋势, 也促使着 XRF 技术在地学领域朝着更加广阔和更多维度发展。XRF 相关新技术, 如微区 XRF、X 射线吸收谱和便携式 XRF 等开始发挥越来越重要的作用, 为 XRF 在地学领域的应用揭开了一种新视野和新机遇。

## Some Difficulties and Status in the Application of X-Ray Spectrometry in Geological Analysis: A Review

YUAN Jing<sup>1</sup>, LI Yingchun<sup>2</sup>, TAN Guili<sup>1</sup>, HUANG Haibo<sup>1</sup>, ZHANG Hua<sup>1\*</sup>, LIU Jiao<sup>1</sup>

(1. Nanjing Center, China Geological Survey, Nanjing 210016, China;

2. National Research Center for Geoanalysis, Beijing 100037, China)

### HIGHLIGHTS

- (1) Preparation of small beads or pellets which are easy to preserve and repeated measurement is the key for quantitative analysis of small size samples and precious samples with XRF.
- (2) The XRF scattering effect can provide a powerful contribution to the analysis of samples with unknown composition and the error correction of the *in situ* analysis of heterogeneous samples.
- (3) Preparation of ultrafine powder pellet, addition of stabilizer and standard addition method establishing work curve are effective approaches for volatile element analysis by XRF.
- (4) Constructing and optimizing the work curve with artificial standard samples or secondary standard samples, preparing low-dilution (sample to flux ratios) glass beads, exciting samples at high X-tube voltage and overcoming overlap interference of spectral lines are effective ways to analyze the rare metals with XRF.

**ABSTRACT:** X-ray fluorescence spectrometry (XRF) has become one of the widely used methods for main and trace elements analysis in geological samples, due to its characteristics of non-destructive, fast, environmentally-friendly and high analytical precision. Currently, XRF can qualitatively and quantitatively analyze most of the major and trace elements (<sup>4</sup>Be–<sup>92</sup>U, especially <sup>10</sup>Na–<sup>92</sup>U) with the concentration ranges from μg/g to percent. However, there are still some difficulties in practical analysis of geological samples with XRF due to the complexity and diversity of mineral composition, physical structural characteristics (e.g. size, shape, delamination and inclusions) and chemical composition (e.g. elemental composition, chemical morphology) of geological samples. This paper elaborates difficulties and corresponding possible solutions of XRF analysis in geological samples from five aspects including small size samples or precious samples analysis, the application of scattering effect, the analysis of volatile elements, variable valence elements and rare metals. Finally, the limitations and challenges of the XRF technique that still exist in the geological analysis are presented. The BRIEF REPORT is available for this paper at <http://www.ykcs.ac.cn/en/article/doi/10.15898/j.ykcs.202403150052>.

**KEY WORDS:** X-ray fluorescence spectroscopy; small size samples and precious samples; scattering effect; volatile elements; variable valence elements; rare metals

### BRIEF REPORT

X-ray fluorescence spectrometry (XRF) analysis of geological samples is often performed using solids or powder, which can avoid the time-consuming complex pretreatment process of wet chemical technology and the use of a large number of toxic and harmful chemical reagents<sup>[2-5]</sup>. Nowadays, XRF has been widely used in the fields of petrology, geochemistry, chronology, mineral resources and environmental geoscience<sup>[9-11]</sup>. However, there are often some difficulties in the practical analysis of geological samples using XRF due to the complexity of geological samples and the characteristics of the elements themselves. Some difficulties and the corresponding possible solutions in geological analysis with the method of XRF are reviewed here, including small size samples or precious samples analysis, the application of scattering effect, the analysis of volatile elements, variable valence elements and rare metals.

### 1. Analysis of small size samples and precious samples

Preparation of small beads or pellets which are easy to preserve and repeated measurement is the key for XRF quantitative analysis of geological samples on a small scale. Sometimes, it is necessary to analyze small size samples or precious samples with XRF, such as meteorites or extraterrestrial samples (for example, lunar samples) as well as banded iron formation<sup>[12]</sup>, loess strata<sup>[13]</sup> and periodically banded rocks within zebra rock<sup>[14]</sup> which can be drilled from banded positions using micro drilling. Such samples can only be qualitative or semi-quantitative by scanning electron microscopy, micro X-ray fluorescence spectrometry or laser ablation-inductively coupled plasma-mass spectrometry as in previous studies. Some researchers have found that preparation of small beads or pellets which are easy to preserve and repeated measurements yield more accurate quantification with XRF.

### 2. Application of the scattering effects

**Scattering effects are used to obtain more information about the chemical composition in samples with unknown elemental composition.** The calibration curve of Compton-to-Rayleigh intensity ratio *versus* average atomic number can provide important information when samples with unknown compositions are studied under the same geometrical conditions and at the same energy. First, construct a calibration curve of Compton-to Rayleigh intensity ratio with respect to the average atomic number using reference materials with well-known chemical composition. Then, the concentration of the elements might be indirectly obtained from scattering X-ray peaks of the samples<sup>[19]</sup>. This method of the evaluation of an unknown specimen is particularly sensitive for a light matrix.

**Scattering effects are beneficial for matrix correction of heterogeneous sample *in situ* analysis.** Researchers have studied the element distribution characteristics of bryophyte-soil-rock interface samples<sup>[20]</sup>. It was found that the correction method with Ray\*Ray/Com is suitable for Ca<sub>K $\alpha$</sub> , Mn<sub>K $\alpha$</sub> , Fe<sub>K $\alpha$</sub> , Cu<sub>K $\alpha$</sub> , Zn<sub>K $\alpha$</sub>  and Pb<sub>L $\alpha$</sub>  whereas the correction with Ray/Com is good for K<sub>K $\alpha$</sub> . When the elements' intensity was corrected by the respective suitable methods, the spectra of K, Ca, Pb, Zn and Cu reached the maximum peaks at the soil layer in interface samples. This exploration is useful for the study of biogeochemical interface processes of the interest elements.

### 3. Analysis of the volatile elements

Volatile elements such as C, S and halogen are difficult to analyze accurately with XRF in both the fusion method and pressed powder pellet in general conditions. The fusion method often leads to the measured value drop. Whereas the measurement accuracy is not ideal either using the pressed powder pellet because of the influence of mineral effect and particle effect. Researchers found that the mineral effect and particle effects can be minimized by ultra-fine grind, and that the uncertainty of the analysis results reduced in response<sup>[21]</sup>. Besides, The addition of stabilizer can inhibit the volatilization of volatile elements such as S at high-temperature in the melting process, so the analytical accuracy can also be improved<sup>[26]</sup>.

### 4. Analysis of the variable valence elements

The characteristic X-ray spectral peak position, and the shape and relative intensity of the spectral line can be affected by the atomic valence states and coordination states<sup>[32-33]</sup>. Some researchers used the relative intensity of Fe K $\beta_2$ /K $\beta_{1,3}$  as an analytical parameter to analyze the content of divalent iron (FeO) in igneous rocks. Chubarov, et al.<sup>[33]</sup> analyzed the valence state and form of manganese in various kinds of manganese ore by S8 Tiger-type wavelength dispersive X-ray fluorescence spectrometer, so that the quality of manganese ore can be accessed quickly without complex processes.

### 5. Analysis of the rare metals

**Constructing and optimizing the work curve with artificial standard samples or secondary standard samples are effective ways to analyze the rare metals with XRF<sup>[36]</sup>.** Zhou et al.<sup>[37]</sup> expanded the work curve linear range of La, Ce and Y by adding high purity rare earth oxides La<sub>2</sub>O<sub>3</sub>, CeO<sub>2</sub> and Y<sub>2</sub>O<sub>3</sub> in the analysis of rare earth minerals and mineralized samples. Silva et al.<sup>[38]</sup> added the secondary standard to establish the work curve and used

the empirical coefficient method to optimize the calibration curve for analysis of La, Ce, Nd, Sm and Gd in Amazon cassiterite tailings. The results of precision and accuracy tests using the CRM (Diorite Gneiss-CCRMP) was satisfactory. Coefficients of variation of five analyzed elements except Gd were less than 5%. The analytical recovery of five elements were between 103% and 116%.

**Preparing low-dilution (sample to flux ratios) glass beads facilitates the determination of rare metals using XRF.** Nakayama et al.<sup>[40]</sup> determined 42 components in felsic rocks using XRF. Low-dilution glass beads with 1 : 1 of sample-to-flux ratios were prepared to measure Sc, Sn, Cs, Hf, Ta and rare earth elements. Calibration curves of the components showed good linearity ( $r=0.991-1.000$ ). Ichikawa et al.<sup>[41]</sup> developed a low-dilution glass-bead method to determine 34 components including rare metals in basaltic and granitic rocks using XRF. The calibration curves present good linearity ( $r>0.990$ ).

**High-energy excitation may help the determination of rare metals in geological samples.** Generally, the L line of rare elements is selected as the analytical line because the K line of rare elements cannot be excited by conventional X-ray tubes. However, high-energy polarization XRF can effectively stimulate the K series of rare metals. The overlap interference of K line of rare metals is less and the excitation factor of the K line is larger than the L line, so the excitation efficiency is greatly improved. Researchers developed a method for multi-element analysis of rare earth elements in soil, rock and deposits using high-energy polarized energy dispersive X-ray fluorescence spectrometer. The excitation voltage of the rare earth elements is up to 100kV. The calibration lines show great linearity (the correlation coefficients  $r>0.99$  for La, Ce, Pr, Nd and Y, the rest of rare earth elements  $r>0.969$ )<sup>[44]</sup>.

**Overlap interference correction of the spectral lines sometimes plays a key role in rare metals analysis**<sup>[42,45]</sup>. For example, Maritz et al.<sup>[45]</sup> analyze the trace elements in soil. There were significant differences between the measured values and recommended values of Hf and Ta elements because of the ignoring of overlap interference between Cu  $K\alpha_1$  lines and Hf  $L\alpha_1$  and Ta  $L\alpha_1$  lines. Some other researchers fully considered the overlap interference of Ta  $L\alpha_1$  (0.1522nm) and Cu  $K\alpha_1$  (0.1541nm) in the determination of Ta, Cs and other rare metals in rocks<sup>[42]</sup>. The measurement bias was not significant according to the criterion of negligible error and student's distributions.

## 6. Challenges and perspectives

The limitations and challenges of the application of XRF technology in geological analysis are still prominent: (1) The accuracy of analysis results depends on standard material, especially for geological samples with complex composition, which requires samples with similar physical and chemical properties to participate in the calibration curve; (2) It is still difficult to quantitatively determine the light elements whose atomic number  $Z<8$ . In the future, with advances in particle physics, optical systems and detection devices, it is believed that these limitations will be overcome. In addition, with the integrated development of earth sciences in recent years, XRF technology has also developed toward a broader and more dimension-focused direction. New technologies related to XRF, such as micro XRF, X-ray absorption spectrum and portable XRF, are playing an increasingly important role in geoscience field.

## 参考文献

- [1] Jalali M, Jalali M. Geochemistry and background concentration of major ions in spring waters in a high-mountain area of the Hamedan (Iran)[J]. *Journal of Geochemical Exploration*, 2016, 165: 49–61.
- [2] Shaltout A A, Castilho I NB, Welz B, et al. Method development and optimization for the determination of selenium in bean and soil samples using hydride generation electrothermal atomic absorption spectrometry[J]. *Talanta*, 2011, 85(3): 1350–1356.
- [3] 陶春军, 李明辉, 马明海, 等. 皖南某典型富硒区土壤-水稻重金属生态风险评估[J]. *华东地质*, 2023, 44(2): 160–171.
- Tao C J, Li M H, Ma M H, et al. Ecological risk assessment of heavy metals in soil-rice in a typical selenium-rich area of southern Anhui Province[J]. *East*

- China Geology*, 2023, 44(2): 160–171.
- [4] 唐志敏, 张晓东, 张明, 等. 新安江流域土壤元素地球化学特征: 来自岩石建造类型的约束[J]. *华东地质*, 2023, 44(2): 172–185.
- Tang Z M, Zhang X D, Zhang M, et al. Geochemical characteristics of soil elements in Xin'an River Basin: Constraints from rock formation types[J]. *East China Geology*, 2023, 44(2): 172–185.
- [5] Oliveira E. Sample preparation for atomic spectroscopy: evolution and future trends[J]. *Journal of the Brazilian Chemical Society*, 2003, 14(2): 174–182.
- [6] 姚泽, 王干珍, 何功秀, 等. X射线荧光光谱法测定锡矿石中锡[J]. *中国无机分析化学*, 2022, 12(6): 48–53.
- Yao Z, Wang G Z, He G X, et al. Determination of tin in tin ore by X-ray fluorescence spectrometry[J]. *Chinese Journal of Inorganic Analytical Chemistry*, 2022, 12(6): 48–53.
- [7] 李迎春, 张磊, 尚文郁. 粉末压片-X射线荧光光谱法分析富硒土壤样品中的硒及主次量元素[J]. *岩矿测试*, 2022, 41(1): 145–152.
- Li Y C, Zhang L, Shang W Y. Determination of selenium, major and minor elements in selenium-rich soil samples by X-ray fluorescence spectrometry with powder pellet preparation[J]. *Rock and Mineral Analysis*, 2022, 41(1): 145–152.
- [8] 闵红, 刘倩, 张金阳, 等. X射线荧光光谱-X射线粉晶衍射-偏光显微镜分析12种产地铜精矿矿物学特征[J]. *岩矿测试*, 2021, 40(1): 74–84.
- Min H, Liu Q, Zhang J Y, et al. Study on the mineralogical characteristics of 12 copper concentrates by X-ray fluorescence spectrometry, X-ray powder diffraction and polarization microscope[J]. *Rock and Mineral Analysis*, 2021, 40(1): 74–84.
- [9] 张敏, 甘黎明, 冯博鑫, 等. 熔融制样-X射线荧光光谱法测定铁矿石中铁、硅、铝[J/OL]. *中国无机分析化学* (2024-07-06) [2024-03-15]. <http://kns.cnki.net/kcms/detail/11.6005.O6.20240701.1017.002.html>.
- Zhang M, Gan L M, Feng B X, et al. Determination of iron, silicon and aluminum in iron ore by X-ray fluorescence spectrometry with fusion sample preparation[J]. *Chinese Journal of Inorganic Analytical Chemistry* (2024-07-06) [2024-03-15]. <http://kns.cnki.net/kcms/detail/11.6005.O6.20240701.1017.002.html>.
- [10] 蒋稟松, 吴龙华, 李柱. 能量色散X射线荧光光谱技术在土壤重金属分析中的应用研究现状[J]. *岩矿测试*, 2024, 43(4): 659–675.
- Jiang A S, Wu L H, Li Z. Application of energy-dispersive X-ray fluorescence spectroscopy in analysis of heavy metals in soil[J]. *Rock and Mineral Analysis*, 2024, 43(4): 659–675.
- [11] 陈春霏, 卢秋, 姚苏芝, 等. 粉末压片-X射线荧光光谱法测定富硅土壤和沉积物样品中的5种重金属元素[J]. *中国无机分析化学*, 2024, 14(5): 513–520.
- Chen C F, Lu Q, Yao S Z, et al. Determination of 5 heavy metal elements in silicon-rich soil sand sediments by X-ray fluorescence spectrometry with pressed powder pellet[J]. *Chinese Journal of Inorganic Analytical Chemistry*, 2024, 14(5): 513–520.
- [12] Li W J, Wang C L, Gao B Y, et al. Determination of multi-element concentrations at ultra-low levels in alternating magnetite and pyrite by HR-ICP-MS using matrix removal and preconcentration[J]. *Microchemical Journal*, 2016, 127: 237–246.
- [13] Zhang W X, Shi Z T, Chen G J, et al. Geochemical characteristics and environmental significance of Taledo loess-paleosol sequences of Ili Basin in central Asia[J]. *Environmental Earth Sciences*, 2013, 70(5): 2191–2202.
- [14] Kelka U, Veveakis M, Koehn D, et al. Zebra rocks: compaction waves create ore deposits[J]. *Scientific Reports*, 2017, 7(1): 1–9.
- [15] Nakayama K, Nakamura T. Undersized (12.5mm diameter) glass beads with minimal amount (11mg) of geochemical and archeological siliceous samples for X-ray fluorescence determination of major oxides[J]. *X-Ray Spectrometry*, 2012, 41(4): 225–234.
- [16] Ichikawa S, Nakamura T. X-ray fluorescence analysis with micro glass beads using milligram-scale siliceous samples for archeology and geochemistry[J]. *Spectrochimica Acta Part B: Atomic Spectroscopy*, 2014, 96: 40–50.
- [17] Gazulla M F, Vicente S, Orduna M, et al. Chemical analysis of very small-sized samples by wavelength-dispersive X-ray fluorescence[J]. *X-Ray Spectrometry*, 2012, 41(3): 176–185.
- [18] Shakhreet B Z, Bauk S, Shukri A. Electron density of *Rhizophora spp.* wood using Compton scattering technique at 15.77, 17.48 and 22.16keV XRF energies[J]. *Radiation Physics and Chemistry*, 2015, 107: 199–206.

- [19] Hodoroaba V, Rackwitz V. Gaining improved chemical composition by exploitation of Compton-to-Rayleigh intensity ratio in XRF analysis[J]. *Analytical Chemistry*, 2014, 86(14): 6858–6864.
- [20] Shen Y T, Luo L Q, Song Y F, et al. Matrix correction with Compton to Rayleigh ratio in a plant-soil-rock interface analysis using a laboratory micro-XRF[J]. *X-Ray Spectrometry*, 2019, 48(5): 536–542.
- [21] 马景治, 肖伟, 向兆, 等. 超细粉末压片-X射线荧光光谱法测定土壤和沉积物中21种主微量元素[J]. *分析试验室*, 2025, 44(1): 29–35.  
Ma J Z, Xiao W, Xiang Z, et al. Determination of major and trace elements in soil and sediment by X-ray fluorescence spectrometry with ultra-fine powder pressing[J]. *Chinese Journal of Analysis Laboratory*, 2025, 44(1): 29–35.
- [22] 彭桦, 罗昆义, 张树洪, 等. 超细样品压片 X 射线荧光光谱分析沙特阿拉伯磷矿中多元素含量[J]. *磷肥与复肥*, 2018, 33(7): 39–42.  
Peng H, Luo K Y, Zhang S H, et al. Analysis of multi-elements in phosphorus rock of Saudi Arabia by XRF ultra-fine sample squash method[J]. *Phosphate & Compound Fertilizer*, 2018, 33(7): 39–42.
- [23] 曾江萍, 李小莉, 张莉娟, 等. 超细粉末压片 X 射线荧光光谱法分析铬铁矿中的多种元素[J]. *矿物学报*, 2015, 35(4): 545–549.  
Zeng J P, Li X L, Zhang L J, et al. Determination of multi-elements in chromite by X-ray fluorescence spectrometry with ultra-fine powder tableting[J]. *Acta Mineralogica Sinica*, 2015, 35(4): 545–549.
- [24] 曾江萍, 张莉娟, 李小莉, 等. 超细粉末压片-X 射线荧光光谱法测定磷矿石中 12 种组分[J]. *冶金分析*, 2015, 35(7): 37–43.  
Zeng J P, Zhang L J, Li X L, et al. Determination of twelve components in phosphate ore by X-ray fluorescence spectrometry with ultra-fine powder tableting[J]. *Metallurgical Analysis*, 2015, 35(7): 37–43.
- [25] 李小莉, 安树清, 徐铁民, 等. 超细粉末压片制样 X 射线荧光光谱测定碳酸岩样品中多种元素及 CO<sub>2</sub>[J]. *光谱学与光谱分析*, 2015, 35(6): 1741–1745.  
Li X L, An S Q, Xu T M, et al. Ultra-fine pressed powder pellet sample preparation XRF determination of multi-elements and carbon dioxide in carbonate[J]. *Spectroscopy and Spectral Analysis*, 2015, 35(6): 1741–1745.
- [26] Gazulla M F, Gomez M P, Orduna M, et al. New methodology for sulfur analysis in geological samples by WD-XRF spectrometry[J]. *X-Ray Spectrometry: An International Journal*, 2009, 38(1): 3–8.
- [27] Li X L, Wang Y M, Zhang Q. Determination of halogen levels in marine geological samples[J]. *Spectroscopy Letters*, 2016, 49(3): 151–154.
- [28] Tiwari M, Sahu S K, Bhargare R C, et al. Depth profile of major and trace elements in estuarine core sediment using the EDXRF technique[J]. *Applied Radiation and Isotopes*, 2013, 80: 78–83.
- [29] Obhodaš J, Valković V, Matjačić L, et al. Evaluation of elemental composition of sediments from the Adriatic Sea by using EDXRF technique[J]. *Applied Radiation and Isotopes*, 2012, 70(7): 1392–1395.
- [30] Abderrahim H, Candela L, Queralt I, et al. X-ray fluorescence analysis for total bromine tracking in the vadose zone: Results for Mnsara, Morocco[J]. *Vadose Zone Journal*, 2011, 10(4): 1331–1335.
- [31] Pashkova G V, Aisueva T S, Finkelshtein A L, et al. Analytical approaches for determination of bromine in sediment core samples by X-ray fluorescence spectrometry[J]. *Talanta*, 2016, 160: 375–380.
- [32] Chubarov V M, Finkelshtein A L. Determination of divalent iron content in igneous rocks of ultrabasic, basic and intermediate compositions by a wavelength-dispersive X-ray fluorescence spectrometric method[J]. *Spectrochimica Acta Part B: Atomic Spectroscopy*, 2015, 107: 110.
- [33] Chubarov V M, Suvorova D, Mukhetdinova A, et al. X-ray fluorescence determination of the manganese valence state and speciation in manganese ores[J]. *X-Ray Spectrometry*, 2015, 44(6): 436.
- [34] Medeiros C A D, Trebat N M. Transforming natural resources into industrial advantage: The case of China's rare earths industry[J]. *Brazilian Journal of Poultry Science*, 2017, 37(3): 504–526.
- [35] Jyothi R K, Thenepalli T, Ahn J W, et al. Review of rare earth elements recovery from secondary resources for clean energy technologies: Grand opportunities to create wealth from waste[J]. *Journal of Cleaner Production*, 2020: 122048.
- [36] 钟坚海. 熔融制样-X 射线荧光光谱法测定铝矿中 15

- 种组分[J]. *冶金分析*, 2018, 38(11): 24–29.
- Zhong J H. Determination of fifteen components in aluminum ore by X-ray fluorescence spectrometry with fusion sample preparation[J]. *Metallurgical Analysis*, 2018, 38(11): 24–29.
- [37] 周伟, 曾梦, 王健, 等. 熔融制样-X 射线荧光光谱法测定稀土矿石中的主量元素和稀土元素[J]. *岩矿测试*, 2018, 37(3): 298–305.
- Zhou W, Zeng M, Wang J, et al. Determination of major and rare earth elements in rare earth ores by X-ray fluorescence spectrometry with fusion sample preparation[J]. *Rock and Mineral Analysis*, 2018, 37(3): 298–305.
- [38] Silva C D, Santana G P, Paz S P A. Determination of La, Ce, Nd, Sm, and Gd in mineral waste from cassiterite beneficiation by wavelength-dispersive X-ray fluorescence spectrometry[J]. *Talanta*, 2020, 206: 120254.
- [39] Price J R, Heitmann N, Hull J, et al. Long-term average mineral weathering rates from watershed geochemical mass balance methods: Using mineral modal abundances to solve more equations in more unknowns[J]. *Chemical Geology*, 2008, 254(1–2): 36–51.
- [40] Nakayama K, Shibata Y, Nakamura T. Glass beads/X-ray fluorescence analyses of 42 components in felsic rocks[J]. *X-Ray Spectrometry: An International Journal*, 2007, 36(2): 130–140.
- [41] Ichikawa S, Onuma H, Nakamura T. Development of undersized (12.5mm diameter) low-dilution glass beads for X-ray fluorescence determination of 34 components in 200mg of igneous rock for applications with geochemical and archeological silicic samples[J]. *X-Ray Spectrometry*, 2016, 45(1): 34–47.
- [42] Suvorova D, Khudonogova E, Revenko A. X-ray fluorescence determination of Cs, Ba, La, Ce, Nd, and Ta concentrations in rocks of various composition[J]. *X-Ray Spectrometry*, 2017, 46(3): 200–208.
- [43] Orescanin V, Mikelic L, Roje V, et al. Determination of lanthanides by source excited energy dispersive X-ray fluorescence (EDXRF) method after preconcentration with ammonium pyrrolidine dithiocarbamate (APDC) [J]. *Analytica Chimica Acta*, 2006, 570(2): 277–282.
- [44] 袁静, 沈加林, 刘建坤, 等. 高能偏振能量色散 X 射线荧光光谱仪测定地质样品中稀土元素[J]. *光谱学与光谱分析*, 2018, 38(2): 582–589.
- Yuan J, Shen J L, Liu J K, et al. Determination of rare earth elements in geological samples by high-energy polarized energy-dispersive X-ray fluorescence spectrometry[J]. *Spectroscopy and Spectral Analysis*, 2018, 38(2): 582–589.
- [45] Maritz H, Cloete H, Elsenbroek J H. Analysis of high density regional geochemical soil samples at the council for geoscience (South Africa): The importance of quality control measures[J]. *Geostandards and Geoanalytical Research*, 2010, 34(3): 265–273.